Neuro-Oncology

Neuro-Oncology 18(4), 538–548, 2016
doi:10.1093/neuonc/nov155
Advance Access date 8 August 2015

Loss of endothelial programmed cell death 10 activates glioblastoma cells and promotes tumor growth

Yuan Zu[†], Kai Zhao[†], Anja Prinz, Kathy Keyvani, Nicole Lambertz, Ilonka Kreitschmann-Andermahr, Ting Lei, and Ulrich Sure

Department of Neurosurgery, University of Duisburg-Essen, Essen, Germany (Y.Z., K.Z., A.P., N.L., I.K.-A., U.S.); Institute of Neuropathology, University of Duisburg-Essen, Essen, Germany (K.K.); Department of Neurosurgery, Tongji Medical College, Wuhan, China (K.Z., T.L.)

Corresponding Author: Yuan Zhu, PhD, Department of Neurosurgery, University of Duisburg-Essen, Hufelandstraße 55, 45122, Essen, Germany (yuan.zhu@uk-essen.de).

[†]equal contribution.

Background. Neo-angiogenesis is a hallmark of glioblastoma (GBM) and is sustained by autocrine and paracrine interactions between neoplastic and nonneoplastic cells. Programmed cell death 10 (PDCD10) is ubiquitously expressed in nearly all tissues and plays crucial roles in regulating angiogenesis and apoptosis. We recently discovered the absence of PDCD10 expression in the tumor vessels of GBM patients. This raised the hypothesis that loss of endothelial PDCD10 affected GBM cell phenotyping and tumor progression.

Methods. Endothelial *PDCD10* was silenced by siRNA and lentiviral shRNA. The tumor cell phenotype was studied in direct and indirect co-culture of endothelial cells (ECs) with U87 or LN229. Angiogenic protein array was performed in the media of *PDCD10*-silenced ECs. Tumor angiogenesis and tumor growth were investigated in a human GBM xenograft mouse model.

Results. Endothelial silence of *PDCD10* significantly stimulated tumor cell proliferation, migration, adhesion, and invasion and inhibited apoptosis in co-cultures. Stable knockdown of endothelial *PDCD10* increased microvessel density and the formation of a functional vascular network, leading to a 4-fold larger tumor mass in mice. Intriguingly, endothelial deletion of *PDCD10* increased ($\geq$2-fold) the release of 20 of 55 tested proangiogenic factors including VEGF, which in turn activated Erk1/2 and Akt in GBM cells.

Conclusions. For the first time, we provide evidence that loss of endothelial *PDCD10* activates GBM cells and promotes tumor growth, most likely via a paracrine mechanism. PDCD10 shows a tumor-suppressor-like function in the cross talk between ECs and tumor cells and is potentially implicated in GBM progression.

Keywords: angiogenesis, endothelial cells, glioblastoma, PDCD10/CCM3.

Glioblastoma (GBM) is the most malignant primary brain tumor, and the median survival of GBM patients remains <15 months despite the combination of surgical resection, radiotherapy, and chemotherapy. Hyper-angiogenesis is a hallmark of GBM and is associated with a high risk of tumor recurrence, disseminated invasive growth, and multitherapy resistance.[1] Thus, targeting tumor angiogenesis has become a promising concept for GBM treatment.[2,3] Growth factors including VEGF are often deregulated in GBM, which contributes to massive neoangiogenesis and tumor progression through multiple downstream pathways such as Ras/Raf, MAPK/Erk, and PI3K/Akt signaling. Preclinical data indicate that targeting these angiogenic growth factors effectively inhibits tumor growth. However, the currently available anti-angiogenic drugs cannot improve the survival of GBM patients.[3] Therefore, the development of new drugs, which target the frequent genetic alterations and complex signaling cross talks between growth factors involved in GBM progress, needs to be considered.

Programmed cell death 10 (PDCD10) was initially named *TFAR15 (TF-1 cell apoptosis related gene 15)*. This gene encodes an evolutionarily conserved protein that is widely expressed in nearly all human tissues and various types of cells including endothelial cells (ECs).[4] Increasing evidence indicates the cell type-dependent apoptotic function of PDCD10.[5–8]

Received 23 March 2015; accepted 15 July 2015

Interestingly, an upregulation of *PDCD10* was identified in response to chemotherapy in various cancers,[9,10] suggesting a possible involvement of PDCD10 in the sensitivity of tumor chemotherapy.

PDCD10 is also known as *cerebral cavernous malformation 3 (CCM3)*. Loss-of-function mutations of *PDCD10* cause human familial cerebral cavernous malformations (CCMs), one of the most common vascular lesions in the central nervous system involving aberrant angiogenesis.[11] CCM patients harboring a *PDCD10* mutation displayed earlier onset of brain hemorrhage[12] than other cavernoma patients, which was associated with the hyperactivation of RhoA kinase.[13,14] PDCD10 is an adaptor protein and can interact with a variety of cytoskeletal and signaling proteins (see recent reviews[15,16]), thereby regulating multiple endothelial functions. Overexpression of *PDCD10* inhibited endothelial proliferation, migration, and tube formation.[7] Silencing *PDCD10* in ECs did the opposite.[17] *Pdcd10* deletion in zebrafish[18] or in mice[19,20] induced abnormal cardiac and cranial vasculature. Beside its apoptotic and angiogenic functions, PDCD10 is also essential for neuronal migration[21] and is involved in the interaction of neuron-ECs and glial cell ECs.[22] Interestingly, Guerrero et al.[23] recently reported that *PDCD10* deletion shows defect autophagy of aging cells and bypasses oncogene-induced cell senescence. PDCD10 has also been implicated in brain tumors. Patients harboring heterozygous mutations of *PDCD10* displayed a high risk of developing meningioma,[12,24,25] suggesting a potential tumor suppressor-like function of PDCD10.

In our group, we have continuously studied the angiogenic and apoptotic functions of PDCD10 in ECs and the underlying pathways.[8,17] We recently observed a significant downregulation of PDCD10 in GBM. Moreover, PDCD10 expression was absent in the ECs of tumor vessels of GBM patients (data have been submitted for publication). We therefore assumed that endothelial deficiency in PDCD10 affected GBM cell phenotyping and tumor progression. Here we report for the first time that endothelial knockdown of *PDCD10* stimulates GBM cell phenotyping towards a more aggressive status in vitro and promotes tumor angiogenesis and tumor growth in vivo through a paracrine mechanism.

Materials and Methods

Cell Culture

Human umbilical vein endothelial cells (HUVECs) were purchased from PromoCell and cultured in endothelial cell growth medium with supplements (Promocell). Two human GBM cell lines, U87 and LN229 (kind gift from the Institute of Cell Biology at our university), were cultured in Dulbecco's modified Eagle's medium containing fetal bovine serum (FBS, 10%) and sodium pyruvate (1%).

Silencing PDCD10 *by siRNA and shRNA*

Specific siRNA targeting human *PDCD10* (siPDCD10) and control siRNA (Neg.C) were obtained from Applied Biosystems/Ambion. Silencing *PDCD10* was achieved by transfection with the best siPDCD10 selected from 3 different siPDCD10s according to a previously established protocol.[8] TRIPZ lentiviral shRNA vector for human *PDCD10* (shPDCD10, Clone ID: V2THS_217165) and empty vector (EV, catalog# RHS4750) were obtained from Thermo Scientific. Lentiviruses were produced by co-transfecting shPDCD10 or EV with trans-lentiviral packaging system in HEK293 cells according to the manufacturer's instruction. The media containing lentiviral-shPDCD10 or -EV were used to perform transduction in HUVECs. After selection with puromycin (1 mg/mL), shRNA expression was induced by the treatment of transduced cells with doxycycline (1 mg/mL).

Direct- and Indirect Co-culture

For direct co-culture, green fluorescent protein (GFP) labelled U87 (U87:GFP) and LN229 (LN:GFP) were respectively co-cultured with HUVECs transfected with either siPDCD10 or Neg.C in a proper ratio optimized in individual experiments. In indirect co-culture, U87 and LN229 were individually cultured with the conditioned medium (CM) and control medium (C) obtained respectively from HUVECs 72 hours after the transfection with siPDCD10 or Neg.C. The phenotype of U87 and LN229 were studied after certain periods of co-cultures as indicated in individual experiments.

Cell Proliferation and Migration

Cell proliferation assay, scratch assay, and transwell migration assay were performed as described previously.[8,17] For spheroid migration assay, U87:GFP- or LN:GFP-spheroid was performed after overnight incubation with 20% methylcellulose solution. The spheroids were reseeded into the plate, which had been precoated with Matrigel. The spheroid diameter was measured at different time points by Image J software.

Cell Invasion and Gelatin Zymography

For transwell invasion assay, GBM cells prestimulated with CM or control medium were suspended in serum-free medium and seeded into the insert, which had been precoated with Matrigel. The medium containing 10% FBS was added into the lower chamber. After incubation for 24 hours, the uninvaded cells were gently removed with a cotton swab. The invaded cells were stained with crystal violet (0.5%) and destained with sodium dodecylsulfate (1%) followed by measuring the absorbance at 550 nm with a plate reader. Meanwhile, to detect pro-MMP2 and MMP2 by gelatin zymography, the media from CM- or control medium-treated GBM cells were collected and loaded into 8% acrylamide gels containing gelatin (0.1%). After electrophoresis, the gels were washed with a buffer containing Triton X-100 (2.5%) and incubated with incubation buffer ($CaCl_2$ 10 mM, $ZnCl_2$ 1 μM, tris 50 mM, pH = 7.6) at 37°C for 20 hours followed by Coomassie blue staining and destaining. The activity of pro-MMP2 and MMP2 was visualized as transparent bands on the blue gels.

Cell Adhesion

For extracellular matrix (ECM) adhesion assay, cells were seeded in a 96-well plate precoated with Matrigel and incubated for 90 minutes. After gently removing the nonadherent cells, the adherent cells were detected after crystal-violet staining.

For vascular adhesion assay, the monolayer of HUVECs was built up on 96-well-plates followed by seeding U87:GFP or LN:GFP (1.0×10^4) on the second day. After 30 minutes of incubation, the non-adherent cells were removed, and the adherent cells were detected by measuring green fluorescence intensity by the plate reader.

Apoptosis Detection

The LN229 cells were treated with 100 nM of staurosporine (STS, Sigma-Aldrich) or 500 μM of $CoCl_2$ (Sigma-Aldrich) for 4 hours and 24 hours, respectively. Apoptotic cells were examined after Hoechst-33258 staining and TUNEL (Merck Millipore). Additionally, active caspase-3 was detected by immunofluorescent staining with the antibody specifically against cleaved caspase-3 (1:400, Cell Signaling Technology) and by a caspase-3 colorimetric protease assay kit (Life Technology).

Western Blot

Total protein extraction and Western blot were performed as described previously.[8] The following antibodies were used: PDCD10 (1:400; Atlas Antibodies); p-Akt, p-Erk1/2, Akt, Erk1/2, and GAPDH (each 1:1000 dilution, Cell Signaling Technology).

Protein Array

Protein array was performed by using a human angiogenesis array kit (R&D Systems) containing 2 membranes. Each membrane was identically precoated with antibodies against 55 different angiogenic proteins, and each protein was detected in duplicate. These 2 membranes were respectively incubated with CM or control medium. The semiquantification of the dots was performed according to the manufacturer's instruction.

Immunofluorescent Staining

Immunofluorescent staining was done according to the protocol described previously.[26] For double-staining, the following antibody mixtures were applied to the sections from xenograft tumor: mouse anti-CD31 (1:40, Dako) and rabbit anti-PDCD10 (1:100, Atlas Antibodies); mouse anti-GFAP (1:200, Sigma-Aldrich) and rabbit anti-p-Erk1/2 (1:200, Cell Signaling Technology); mouse anti-GFAP (1:200) and rabbit anti-p-Akt (1: 200, Cell Signaling Technology); mouse anti-PCNA (1:200, Dako) and rabbit anti-vWF (1:500, Dako); and mouse anti-PCNA (1:200) and rabbit anti-GFAP (1:500, Dako). Negative control sections were incubated with nonimmune IgG. Counterstaining was performed with Hoechst-33258. The images were acquired using a fluorescence microscope (Axio Imager M2, Zeiss).

Glioblastoma Xenograft Model and Treatment

The animal experiments were performed strictly according to the ethics contract (Nr.: 84-02.04.2012.A348). A GBM xenograft model was established using female nude mice (4–6 weeks old). This model consisted of 3 main steps: (i) spheroid formation by the mixture of U87 and shPDCD10-transduced HUVECs (shPDCD10-HUVEC) or U87 and EV-transduced HUVECs (EV-HUVEC) in a ratio of 1:1; (ii) for plug preparation, 500 spheroids were suspended in a Matrigel-fibrin matrix containing VEGF and bFGF (each 1000 ng/mL, R&D Systems); (iii) the plug was subcutaneously implanted into the flank of the mice as described previously.[27] To maintain the stable knockdown of *PDCD10* in vivo, the mice were served their drinking water containing doxycycline (2 mg/mL) and sucrose (1%). To investigate whether inhibition of VEGF signaling could rescue shPDCD10-induced tumor growth, the mice implanted with U87 and shPDCD10-HUVECs were treated daily with AZD2171 (AZD, MedChem Express), a pan-VEGF receptor tyrosine kinase inhibitor (3 mg/kg, i.g.) beginning on the sixth day of implantation for 14 days. The control mice received the vehicle treatment (the same volume of 1% polysorbate-80). The tumor size was inspected twice a week by using a caliper. The tumor volume (V_T) was calculated according to previous description.[28] The xenograft tumors were removed from the mice for further studies 20 days after implantation.

To evaluate the microvessel density (MVD), immunofluorescent staining of CD31 (1:40, Dako) was performed on the sections from the xenograft tumor. The hotspot method was used for MVD evaluation as described in our previous publication.[26]

Statistical Analysis

Statistical analysis was performed using WinSTAT program. Results between 2 groups were analyzed by the Student *t* test. Differences between multiple groups were analyzed by using ANOVA followed by the Schaeffer test. A P value $<.05$ was considered statistically significant.

Results

Direct and Indirect Co-culture of Glioblastoma Cells With PDCD10*-silenced Endothelial Cells Stimulated Tumor Cell Phenotyping*

In the direct co-culture experiment, U87:GFP and LN:GFP grew significantly faster after co-culture with *PDCD10*-silenced HUVECs (siPDCD10-HUVEsC) than with control HUVECs (C) ($P < .001$) (Fig. 1A), respectively. In both ECM adhesion (Fig. 1B-a) and vascular adhesion assays (Fig. 1B-b), U87:GFP or LN:GFP co-cultured with siPDCD10-HUVECs displayed a higher adhesion ability compared with the corresponding controls ($P < .001$ and $P < .01$, respectively, for U87:GFP and LN:GFP in ECM adhesion; $P < .001$ for both U87:GFP and LN:GFP cells in vascular adhesion). The mobility of both types of GBM cells was also markedly accelerated after co-culture with siPDCD10-HUVECs as demonstrated by scratch assay (Fig. 1C-a) and spheroid migration assay (Fig. 1C-b) ($P < .001$ for both types of GBM cells and both methods). These data indicate that silencing *PDCD10* in ECs stimulates phenotyping GBM cells toward to an active status in a direct co-culture model.

In the indirect co-culture model, WST-1 assay demonstrated 31% ($P < .001$) and 58% ($P < .001$) increase in the proliferation of U87 and LN229, respectively, after incubation with CM compared with the corresponding controls (Fig. 2A). Treatment of U87 and LN229 with CM also significantly promoted the adhesion of both GBM cells ($P < .01$) (Fig. 2B).

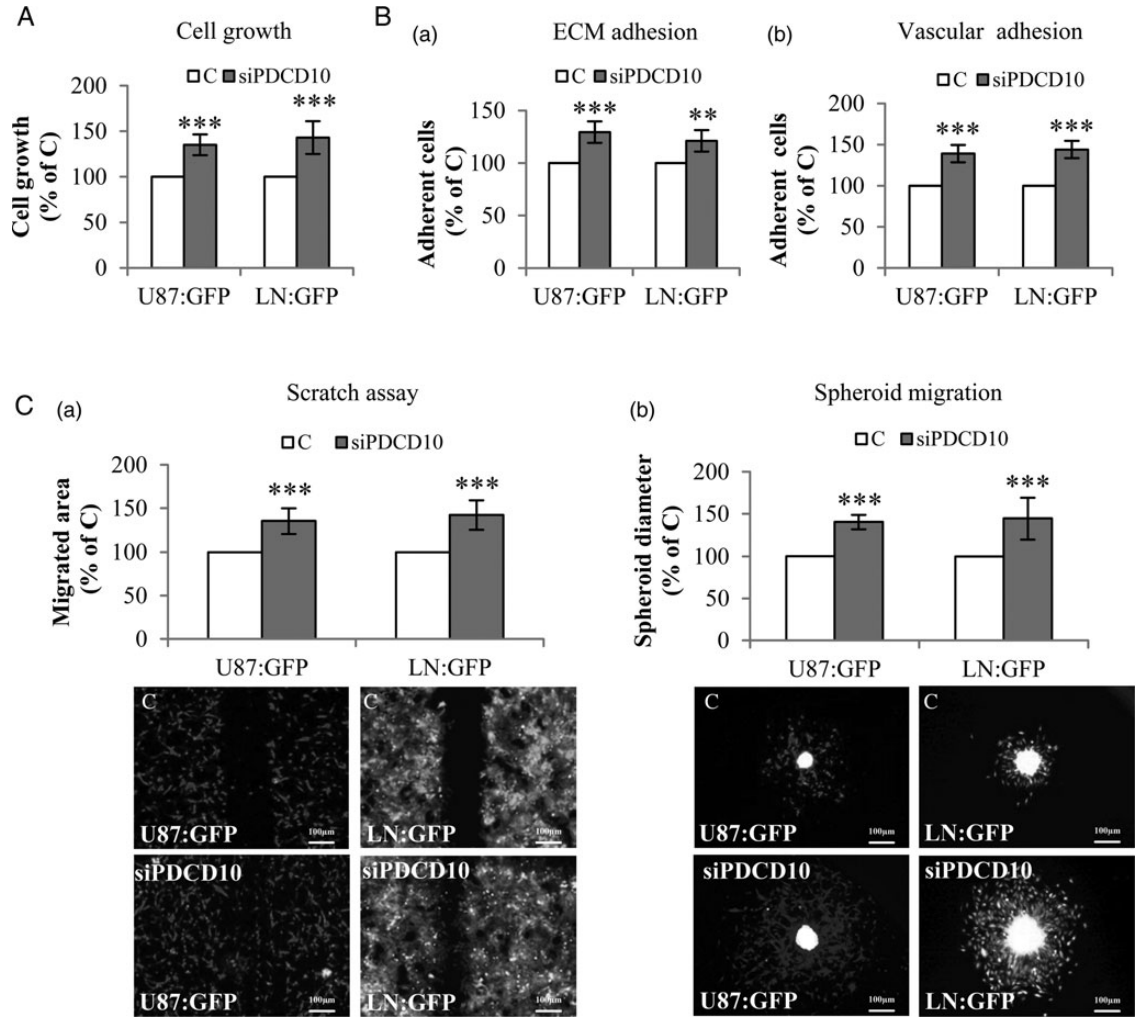

Fig. 1. Direct co-culture of glioblastoma (GBM) cells with *PDCD10*-silenced human umbilical vein endothelial cell (HUVEC)-activated tumor phenotyping. HUVECs were transfected with either siPDCD10 or control siRNA (C) and used for direct co-culture with GBM cells (U87:GFP or LN:GFP) after 72 hours of the transfection. (A) Endothelial silence of *PDCD10* promoted GBM cell growth. The growth of U87:GFP or LN:GFP was detected as green fluorescent intensity at 485 nm of excitation wavelength and 535 nm of emission wavelength. (B) Endothelial silence of *PDCD10* facilitated extracellular matrix (ECM) adhesion (a) and vascular adhesion (b) of GBM cells. The adherent U87:GFP or LN:GFP cells were quantified by detecting green fluorescent intensity of cells. (C) Endothelial silence of *PDCD10* stimulated GBM cell migration. For scratch assay (a), the migrated area was calculated by subtracting the open area at zero hour from that measured at 24 hours after scratching. For spheroid migration assay (b), the diameter of spheroids was measured at 36 hours after seeding spheroids containing HUVECs and GBM cells. ** $P < .01$ and *** $P < .001$, compared to C. Scale bar: 100 μm.

A dramatically enhanced invasion of U87 and LN229 was observed after incubation with CM. The invaded cells increased by 66% ($P < .001$) and 105% ($P < .001$) in CM-treated U87 and LN229 compared with the corresponding controls, respectively (Fig. 2C-a). Moreover, a mildly, but significantly, increased level of MMP2 protein was detected in the medium of CM-treated U87 and LN229 (both $P < .01$) (Fig. 2C-b). These data suggest that incubation of GBM cells with CM accelerates GBM cell invasion, which is associated with the activation of MMP2. Furthermore, a remarkable increase in the migration of GBM cells was observed after CM treatment as demonstrated in scratch assay ($P < .001$) (Fig. 2D-a), spheroid migration assay ($P < .001$) (Fig. 2D-b), and transwell migration assay ($P < .01$) (Fig. 2D-c).

Treatment of Glioblastoma Cells With Conditioned Medium From PDCD10*-Silenced Endothelial Cells Inhibited Caspase-3 Activation and Apoptosis*

Hoechst-33258 staining revealed a 32% ($P < .001$) and 24% ($P < .001$) reduction of apoptotic cells (arrows in Fig. 3A) in CM-treated LN229 after stimulation with STS or $CoCl_2$, respectively. This apoptosis-resistant effect was confirmed by TUNEL staining ($P < .01$) (Fig. 3B). Immunofluorescent staining revealed a significant reduction of the number of active caspase-3-positive LN229 in CM-treated groups (right column in Fig. 3C-a). CM-mediated inhibition of caspase-3 activity in GBM cells was further confirmed by the quantitative assay of caspase-3 enzyme activity ($P < .01$ for both models) (Fig. 3C-b).

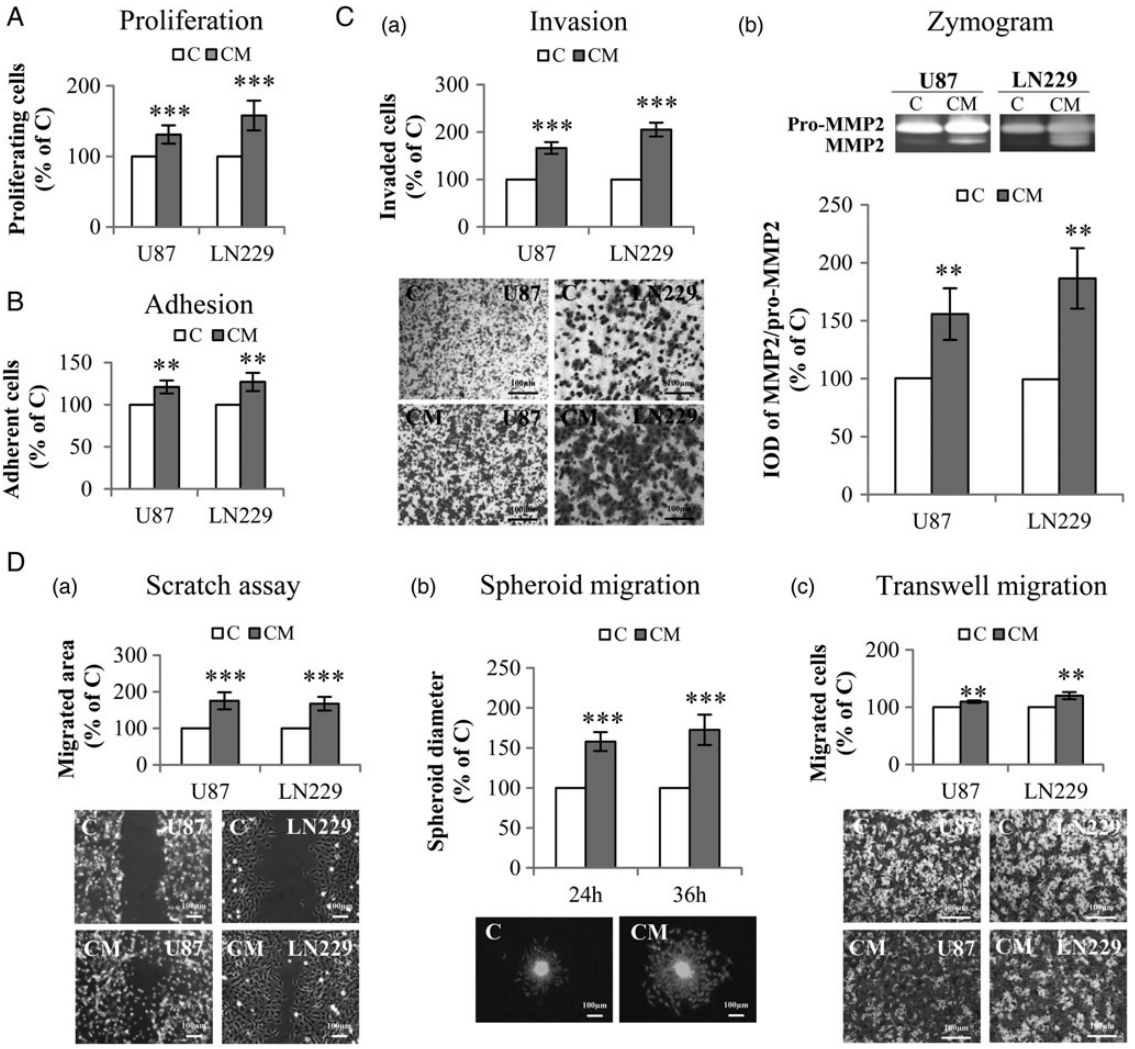

Fig. 2. Indirect co-culture of glioblastoma (GBM) cells with *PDCD10*-silenced human umbilical vein endothelial cells (HUVECs) stimulated GBM cell proliferation, adhesion, invasion, and migration. Indirect co-culture was achieved by the culture of GBM cells with conditioned medium (CM) or with control medium (C), collected from HUVECs at 72 hours after the transfection with siPDCD10 and control siRNA respectively. (A) GBM cell proliferation detected by WST-1 assay. (B) GBM cell adhesion. Cell adhesion was determined by crystal-violet staining followed by measuring the absorbance at 550 nm. (C) CM facilitated invasion of GBM cells (a) accompanied with activation of MMP2 (b). U87 or LN229 were treated with CM or control medium for 24 hours. Prestimulated cells were then seeded in 24-well transwell plates coated with Matrigel. Cell invasion was quantified 24 hours after the incubation by crystal-violet staining (a); meanwhile, the culture medium of prestimulated cells was collected for gelatin zymography (b). (D) GBM cell mobility was measured by scratch assay (a), spheroid migration assay (b), and transwell migration assay (c). For scratch assay (a), cell migration was recorded 10 hours after scratching. To perform spheroid migration assay (b), the spheroids formed by LN:GFP were suspended in CM or in control medium, and seeded on 96-well plates precoated with Matrigel. For transwell migration assay (c), U87 or LN229 were suspended in serum-free medium and added into the insert of 24-well transwell plates. CM or control medium was added into the lower chamber. After incubation for 24 hours, the migrated cells were detected after crystal-violet staining. IOD: integrated optical density. ** $P < .01$ and *** $P < .001$, compare to C. Scale bar: 100 μm.

Endothelial Deletion of PDCD10 *Stimulated Angiogenesis and Tumor Growth in Glioblastoma Xenograft Model*

Before using shPDCD10-HUVECs for the GBM xenograft experiment, the downregulation of PDCD10 in shPDCD10-HUVECs was confirmed at both mRNA ($P < .001$) (Fig. 4A-a) and protein levels ($P < .001$) (Fig. 4A-b). The stable knockdown of PDCD10 in ECs was further confirmed by double-staining PDCD10 and CD31 on the sections from the xenograft tumors. As shown in Fig. 4B, PDCD10 was absent in the microvessels in the section prepared from the mice implanted with U87 and shPDCD10-HUVECs (shPDCD10-mice) (arrows in Fig. 4B-b), whereas PDCD10 was co-expressed with CD31 in the ECs in the control (arrows in Fig. 4B-a). Of note, immunostaining of PCNA showed many more proliferating cells on the section prepared from shPDCD10-mice (Fig. 4C-b) than from the control (Fig. 4C-a). Double-staining further demonstrated that knockdown of *PDCD10* in ECs not only promoted the proliferation of

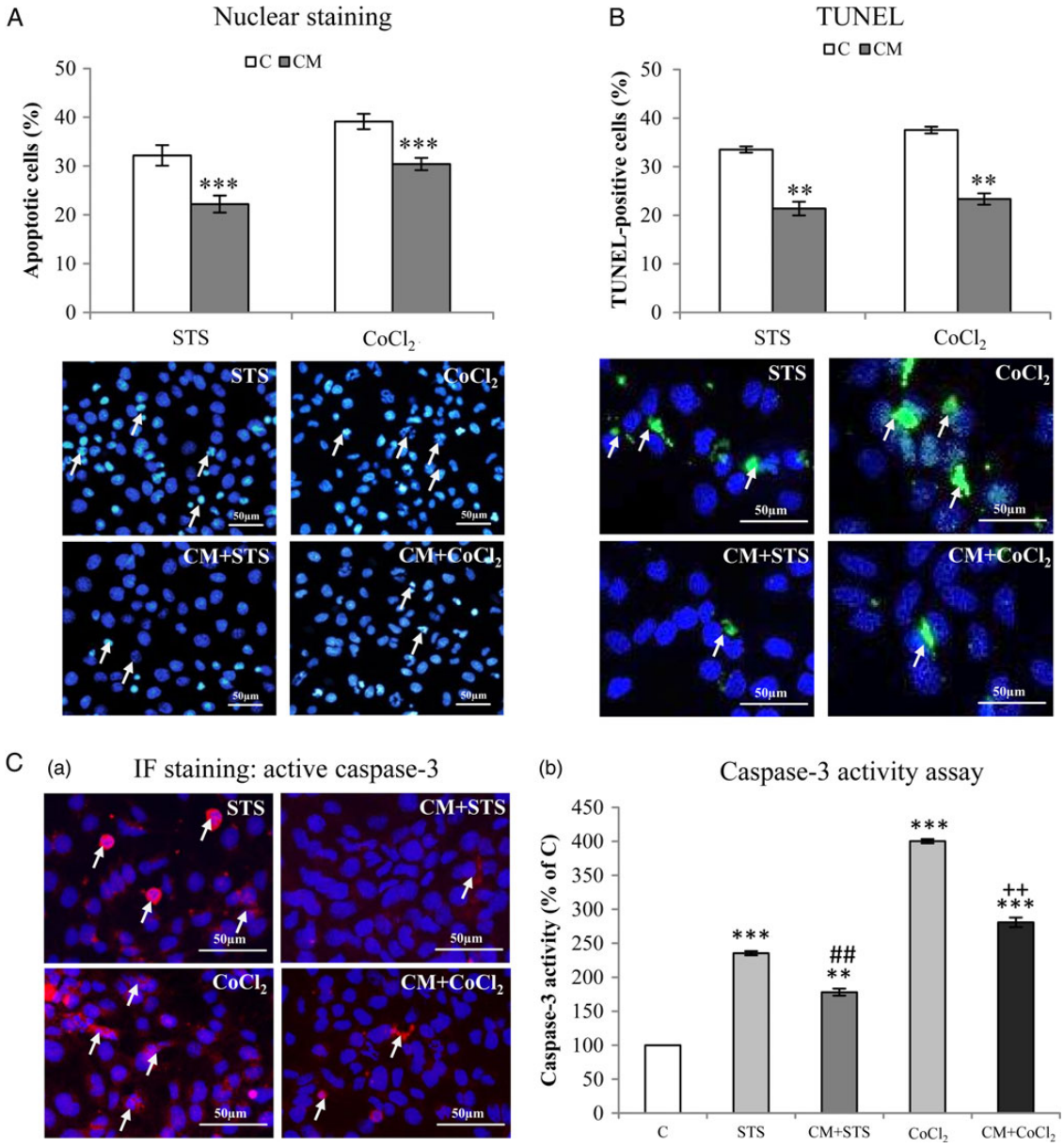

Fig. 3. Indirect co-culture of glioblastoma (GBM) cells with *PDCD10*-silenced human umbilical vein endothelial cells (HUVECs) inhibited activation of caspase-3 and reduced apoptosis in GBM cells. After incubation of LN229 with conditioned medium (CM) or control medium (C) overnight, stausporine (STS, 100nM) and $CoCl_2$ (500 μM) were treated to cells for 4 hours and 24 hours, respectively, followed by Hoechst-33258 staining (A) and Terminal dexynucleotidyl transferase-mediated dUTP nick end labeling (TUNEL) (B). (Arrows indicate apoptotic cells). Active caspase-3 was detected by immunofluorescent staining (C-a, arrows indicated positive-stained cells) and by caspase-3 enzyme activity assay (C-b). ** $P < .01$ and *** $P < .001$, compare to C; ## $P < .01$, compare to STS alone; ++ $P < .01$, compare to $CoCl_2$ alone. Scale bar: 50 μm.

vWF-positive ECs (arrows in Fig. 4C-d) but also stimulated GFAP-positive GBM cell proliferation (arrowheads in Fig. 4C-f). In contrast, proliferating cells were observed at a much lower extent in the controls (Fig. 4C-a, c and e). As revealed by double-staining, a massive activation of Erk1/2 and Akt was exclusively observed in GFAP-positive tumor cells on the sections from shPDCD10-mice implants (arrows in lower panel of Fig. 4D), whereas the immunoreactivity of p-Erk1/2 and p-Akt was only marginally detected in the controls (upper panel of Fig. 4D). Moreover, H&E staining revealed the histological and vascular features of the xenograft tumors comprising numerous tumor cells and microvessels that often contained blood cells (upper panel, Fig. 4E-a), indicating a functional vascular network in xenograft tumors. CD31-immunoflurecent staining demonstrated that deletion of *PDCD10* in ECs not only led to the formation of a more branched microvascular network (lower panel, Fig. 4E-a) but also increased MVD in xenograft ($P < .001$) (Fig. 4E-b). As a consequence, the tumor growth rate was significantly faster in shPDCD10-mice than in the control mice as inspected from days 9–18 after implantation

($P < .01$) (Fig. 4F-b). At 20 days after implantation, the tumor mass in the shPDCD10-mice was 4-fold larger than that in the controls ($P < .001$) (Fig. 4F-a and F-b). Interestingly, the shPDCD10-induced increase in MVD (Fig. 4E) and the aggressive tumor growth rate (Fig. 4F) were completely reversed by treating the mice with AZD, indicating a master role of VEGF in the interaction between *PDCD10*-deficient ECs and GBM cells and in tumor progression.

Endothelial Silence of PDCD10 *Stimulated the Release of Soluble Factors That in Turn Activated Survival Pathways in Glioblastoma Cells*

To address the potential mechanism underlying the pro-angiogeneic and antiapoptotic effects induced by endothelial deletion of *PDCD10*, we performed a protein array of 55 angiogenic factors in conditioned medium from siPDCD10-transfected HUVECs (CM) and in control medium (C). The efficiency of *PDCD10* silence in HUVECs was confirmed simultaneously before the experiment (Fig. 5A-a and b). The dot-blots reflecting the protein expression are shown in Fig. 5B. Semiquantification of the blots revealed that 20 of 55 target proteins showed >2-fold upregulation in CM. These proteins were CD26, EGF, FGF-4, GDNF, GM-CSF, HB-EGF, HGF, Leptin, MIP-1α, MMP-8, MMP-9, NRG1-β1, PD-ECGF, Persephin, CXCL4, Serpin F1, TSP-1, Vasohibin, VEGF, and VEGF-C (Fig. 5C).

We further examined whether CM stimulated GBM cell phenotyping via activation of Erk1/2 and Akt. As shown in Fig. 5D, CM-treated U87 expressed a markedly higher level of p-Erk1/2 and p-Akt than those treated with control medium, which was entirely reversed by the co-treatment with the specific inhibitor U126 (20 μM) or with wortmannin (Wm, 200 nM). These results suggest that the increase in the release of multiple soluble factors in CM was sufficient to activate Erk1/2 and Akt in GBM cells, which is consistent with the observation from immunofluorescent staining on xenograft sections (arrows lower panel of Fig. 4D).

Discussion

PDCD10 is ubiquitously expressed in nearly all tissues. Loss-of-function mutation of *PDCD10* causes CCMs. However, little is known about this protein in malignant tumors despite its original definition as an apoptosis-related protein. We have recently discovered that PDCD10 is significantly downregulated in GBM and, more intriguingly, PDCD10 is absent in the ECs of microvessels in GBM (data have been submitted for publication). Based on the crucial role of PDCD10 in regulating angiogenesis and apoptosis[8,17] and considering the direct interaction of ECs and tumor cells in the pathological circumstance of GBM, the present study investigated the influence of *PDCD10*-deleted ECs on GBM-cell phenotyping and on tumor angiogenesis and tumor growth. Here we provide evidence that endothelial silence of *PDCD10* leads to: (i) the stimulation of GBM cell proliferation, adhesion, migration, and invasion in direct and indirect co-cultures; (ii) the resistance of GBM cells to apoptotic stimuli; (iii) the activation of neo-angiogenesis and tumor growth in human GBM xenograft in mice; and (iv) an increase in the release of 20 proangiogenic and growth factors that in turn activates Erk1/2 and Akt in GBM cells. These findings suggest that PDCD10 functions as a novel tumor suppressor-like molecule and is potentially implicated in the pathology of GBM.

It is known that ECs in GBM have intrinsic properties distinctly different from normal ECs in the brain.[29] Absence of PDCD10 expression in ECs of GBM, as discovered in our recent study, supports this concept. The present study shows that endothelial knockdown of *PDCD10* activates GBM cell proliferation, adhesion, migration, and invasion, which are all critical parameters for tumor progression and risk factors accounting for tumor recurrence and poor prognosis. Because these findings are completely novel, we carefully confirmed the results by applying 2 in vitro models (ie, direct and indirect co-culture with 2 different GBM cell lines and multiple assays for each phenotype study). The data were further strengthened by the xenograft model of GBM, through which the role of *PDCD10*-deleted ECs in tumor neo-angiogenesis and tumor growth was confirmed. In comparison with other xenograft tumor models formed by pure tumor cells, co-implantation of GBM cells together with ECs more appropriately mimicked the reality of tumor microenvironment. Furthermore, unlike the in situ intracranial xenograft model, our model eliminates the influence of other brain components and is thus particularly suitable for study of the putative paracrine effects of genotype-altered ECs on GBM phenotype.

Both autocrine signals through neoplastic cells and paracrine ligands secreted from nonneoplastic cells can create a permissive microenvironment for malignant tumor progression.[30] The interaction between glioma cells and the surrounding microenvironment takes place through direct cell-cell contact and/or the secreted factors from nonneoplastic cells including ECs, active astrocytes, or microglial cells in brain. Numerous factors released from ECs play pivotal roles in regulating tumor cell phenotype, tumor angiogenesis, and tumor progression.[30,31] Here we demonstrate that endothelial deletion of PDCD10 causes the increase in the release of 20 proangiogenic factors among 55 tested proteins (Fig. 5C). Among 20 upregulated factors, many of them (eg, VEGF, GDNF, EGF, and HGF) are well-known growth factors implicated in GBM pathology. Thus, we believe that all of these upregulated factors play synergistic roles in simulating tumor angiogenesis and tumor growth mediated by shPDCD10. Moreover, it is also known that positive regulation loops are often present in the network comprising numerous proangiogenic and growth factors. For example, EGF and FGF have been shown to stimulate VEGF synthesis in GBM;[32] VEGF facilitates other proangiogenic factors such as MMPs.[33] Abolishment of shPDCD10-induced angiogenesis and tumor growth by VEGF receptor inhibitor in mice (Fig. 4E and F) implicates VEGF as a dominant player among these upregulated factors in the interaction between *PDCD10*-deficient ECs and GBM cells and in tumor progression.

PDCD10 silence-induced increase in a group of soluble factors may simultaneously act on endothelial cells and on GBM cells and activate common and diverse signaling pathways. The presence of various growth factor receptors on GBM cells has been previously demonstrated,[34] which makes tumor progression through paracrine mechanism possible. PI3K/Akt and MAPK/Erk1/2 signaling are known as common pathways triggered by growth factors, and both pathways are important for tumor cell proliferation, migration, and invasion as well as

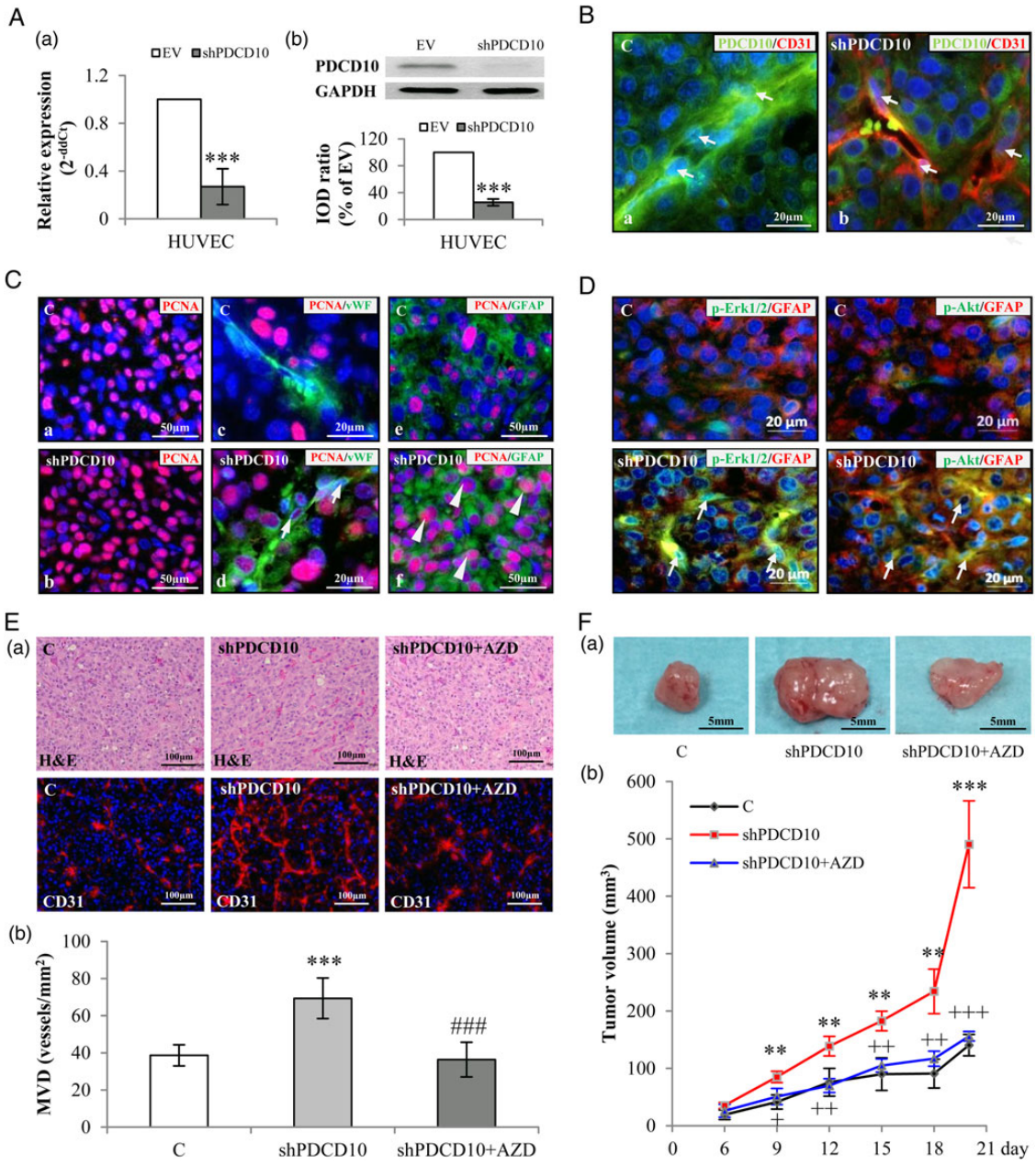

Fig. 4. Endothelial knockdown of *PDCD10* stimulated neo-angiogenesis and tumor growth in a human glioblastoma (GBM) xenograft model in mice. The xenograft tumors were resulted from the mixtures of U87 and EV-transduced human umbilical vein endothelial cells (HUVECs) (C) or U87 and shPDCD10-HUVECs (shPDCD10). shPDCD10 mice (shPDCD10+AZD) were treated with AZD2171 (3 mg/kg, i.g.) beginning on the sixth day of implantation for 14days ($n = 4$); C and shPDCD10 mice received vehicle only ($n = 4$ for each group). The xenograft tumors were removed from the mice after 20 days of implantation. (A) Confirmation of *PDCD10* knockdown at mRNA (a) and protein levels (b) in HUVECs before mice implantation. *** $P < .001$, compare to EV. (B) Stable knockdown of endothelial PDCD10 in xenograft tumors. Double-staining indicated absence of PDCD10 in CD31-positive cells (red) in tumors formed by U87 and shPDCD10-HUVECs (shPDCD10-mice) (arrows in b), whereas co-expression of PDCD10 (green) and CD31 (red) was detected in ECs of tumors formed by U87 and EV-HUVECs (C) (arrows in a). Scale bar: 20 μm. (C) Endothelial knockdown of PDCD10 facilitated tumor cell proliferation. Immunofluorescent staining indicated extensive PCNA immunoreactivity (red) in shPDCD10-mice (b) compared with the control (a). Double staining showed that ECs (arrows in d) and GFAP-positive tumor cells (arrowheads in f) were undergoing a more massive proliferation in shPDCD10-mice as compared with the controls (c and e). Scale bar: 50 μm in a, c, d and f; 20 μm in b and e. (D) Endothelial deletion of *PDCD10* activated Erk1/2 and Akt in xenograft tumor cells. Double-staining demonstrated the activation of Erk1/2 (green) or Akt (green) in GFAP-positive GBM cells (red) of xenograft tumors from shPDCD10-mice (arrows). Scale bar: 20 μm. (E) Endothelial knockdown of PDCD10 stimulated neo-angiogenesis, which was reversed by the treatment of mice with AZD. Both H&E staining and CD31-immunofluorescent staining (a) revealed increased microvessel density (MVD) with more branches in xenograft tumors of shPDCD10-mice compared with control. The neo-angiogenic features induced by shPDCD10 were reversed by AZD treatment. Quantitative

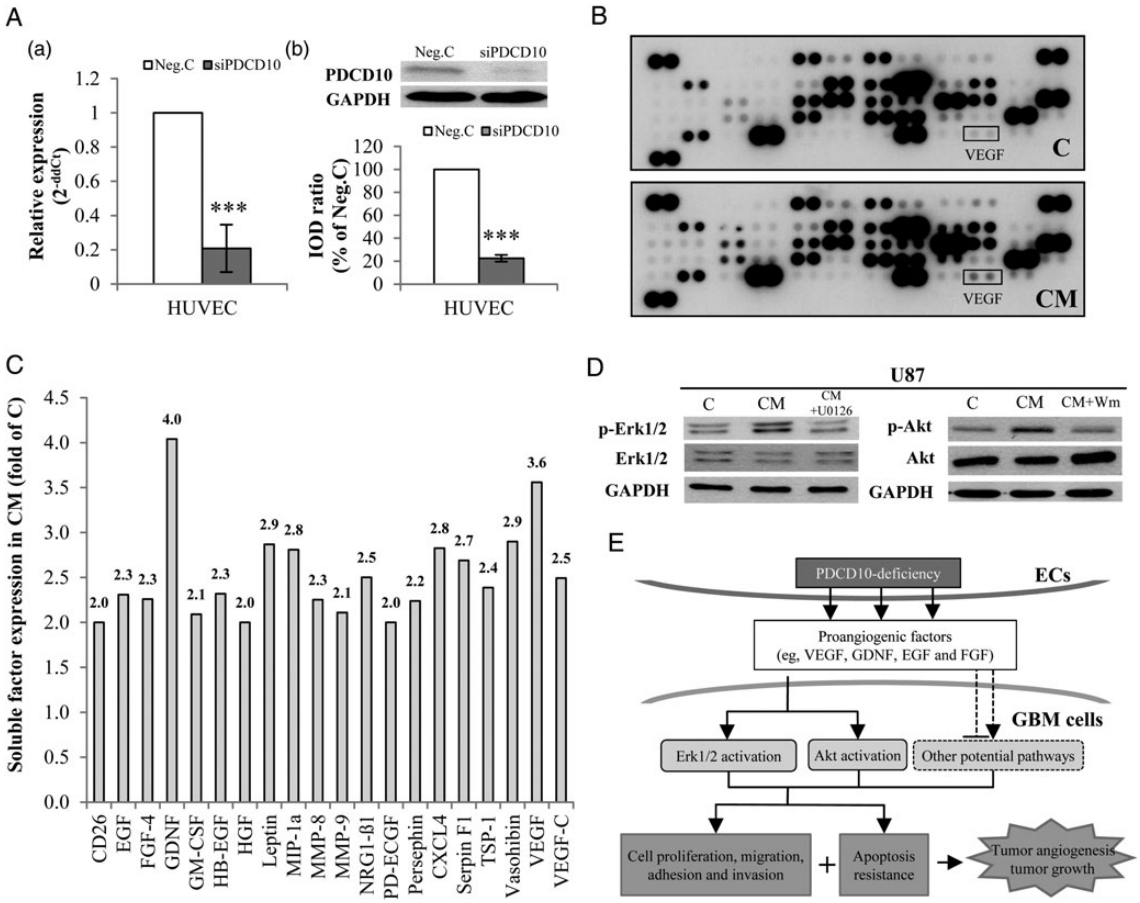

Fig. 5. Endothelial silence of *PDCD10* stimulated the release of proangiogenic factors that in turn activated Erk1/2 and Akt signaling in glioblastoma (GBM) cells. (A) Confirmation of silencing *PDCD10* in human umbilical vein endothelial cells (HUVECs) by RT^2-PCR (a) and Western blot (b) after siRNA transfection. *** $P < .001$, compared with control siRNA (Neg. C). (B) Detection of soluble factors by protein array. The media from siPDCD10- (CM) or Neg.C-transfected HUVECs (C) were collected for protein array. The blots show dots-array of 55 angiogenic factors. Each protein was detected in duplicate. (C) Semiquantification of blots. The expression of all 55 tested angiogenic proteins was semiquantified, and the proteins showing > 2-fold upregulation in CM are presented in this bar graph. (D) Treatment of GBM cells with CM activated Erk1/2 and Akt in GBM cells. Wm: wortmannin. (E) The schematic outline of the influence of *PDCD10*-deleted endothelia on GBM cells. Loss of *PDCD10* in ECs stimulated GBM cells towards a more aggressive phenotype led to apoptosis resistance, activated neo-angiogenesis, and eventually promoted tumor growth. Meanwhile, silence of endothelial *PDCD10* facilitated the release of multiple proangiogenic growth factors and activated Erk1/2 and Akt pathways in GBM cells. Considering the fact that Erk1/2 and Akt signaling pathways are often triggered by growth factors and play an essential role in regulating tumor cell phenotyping and tumor progression, we suppose that the influence of *PDCD10*-deleted endothelia on GBM cells involves a paracrine mechanism.

tumor angiogenesis. Here we demonstrate for the first time that endothelial knockdown of *PDCD10* activates both Akt and Erk1/2 in cultured GBM cells and in xenograft tumor cells (Figs 4D and 5D). Given the underlying promise of the evidence that deletion of *PDCD10* in ECs stimulates GBM cells and promotes tumor angiogenesis and tumor growth, PDCD10 seems to play a crucial role in the context of tumor cells and ECs interacting in GBM.

Numerous proangiogenic and growth factors have been demonstrated as targets of GBM therapy.[2,3] However, drug targeting a single factor has shown limited benefits for GBM patients. Therefore, targeting multiple angiogenic and growth factors is anticipated to be a more effective therapy against tumor progression. Knockdown of *PDCD10* in ECs triggered survival and angiogenic signaling pathways in GBM cells by simultaneously stimulating the release of multiple proangiogenic

analysis of MVD is shown in b. *** $P < .001$, compare to C; ### $P < .001$, compare to shPDCD10. Scale bar: 100 μm. (F) Co-implantation of U87 and shPDCD10-HUVECs promoted tumor growth that was abolished by the treatment of mice with AZD. The representative photos show the tumors from control-, shPDCD10-mice, and AZD-treated shPDCD10-mice on day 20 after implantation (a). Scale bar: 5 mm. The tumor growth curve is shown in b. ** $P < .01$ and *** $P < .001$, compare to C; + $P < .05$, ++ $P < .01$ and +++ $P < .001$, compare to shPDCD10.

and growth factors, thereby stimulating GBM cells and promoting tumor angiogenesis and tumor growth (Fig. 5E). These findings promot PDCD10 as a potential and novel target for future GBM therapy.

Funding

This study was supported financially by the IFORES-program of the Medical Faculty, University of Duisburg-Essen to Y.Z.

Acknowledgments

The authors thank Ms. Rita Haase and Ms. Eva Kusch for technical assistance and Mike Sucker for his assistance in editing the graphics. K.Z. received a scholarship from the Medical Faculty, University of Duisburg-Essen.

Conflict of interest statement. None declared.

References

1. Onishi M, Ichikawa T, Kurozumi K, et al. Angiogenesis and invasion in glioma. *Brain Tumor Pathol*. 2011;28(1):13–24.
2. Cloughesy TF, Cavenee WK, Mischel PS. Glioblastoma: from molecular pathology to targeted treatment. *Annu Rev Pathol*. 2014;9:1–25.
3. De Bonis P, Marziali G, Vigo V, et al. Antiangiogenic therapy for high-grade gliomas: current concepts and limitations. *Expert Rev Neurother*. 2013;13(11):1263–1270.
4. Petit N, Blecon A, Denier C, et al. Patterns of expression of the three cerebral cavernous malformation (CCM) genes during embryonic and postnatal brain development. *Gene Expr Patterns*. 2006;6(5):495–503.
5. Fidalgo M, Guerrero A, Fraile M, et al. Adaptor protein cerebral cavernous malformation 3 (CCM3) mediates phosphorylation of the cytoskeletal proteins ezrin/radixin/moesin by mammalian Ste20–4 to protect cells from oxidative stress. *J Biol Chem*. 2012;287(14):11556–11565.
6. Chen L, Tanriover G, Yano H, et al. Apoptotic functions of PDCD10/CCM3, the gene mutated in cerebral cavernous malformation 3. *Stroke*. 2009;40(4):1474–1481.
7. Schleider E, Stahl S, Wustehube J, et al. Evidence for anti-angiogenic and pro-survival functions of the cerebral cavernous malformation protein 3. *Neurogenetics*. 2011;12(1):83–86.
8. Zhu Y, Wu Q, Xu JF, et al. Differential angiogenesis function of CCM2 and CCM3 in cerebral cavernous malformations. *Neurosurg Focus*. 2010;29(3):E1.
9. Gonzalez-Fernandez R, Morales M, Avila J, et al. Changes in leukocyte gene expression profiles induced by antineoplastic chemotherapy. *Oncol Lett*. 2012;3(6):1341–1349.
10. Aguirre AJ, Brennan C, Bailey G, et al. High-resolution characterization of the pancreatic adenocarcinoma genome. *Proc Natl Acad Sci USA*. 2004;101(24):9067–9072.
11. Bergametti F, Denier C, Labauge P, et al. Mutations within the programmed cell death 10 gene cause cerebral cavernous malformations. *Am J Hum Genet*. 2005;76(1):42–51.
12. Riant F, Bergametti F, Fournier HD, et al. CCM3 Mutations are associated with early-onset cerebral hemorrhage and multiple meningiomas. *Mol Syndromol*. 2013;4(4):165–172.
13. Borikova AL, Dibble CF, Sciaky N, et al. Rho kinase inhibition rescues the endothelial cell cerebral cavernous malformation phenotype. *J Biol Chem*. 2010;285(16):11760–11764.
14. Stockton RA, Shenkar R, Awad IA, et al. Cerebral cavernous malformations proteins inhibit Rho kinase to stabilize vascular integrity. *J Exp Med*. 2010;207(4):881–896.
15. Draheim KM, Fisher OS, Boggon TJ, et al. Cerebral cavernous malformation proteins at a glance. *J Cell Sci*. 2014;127(Pt 4):701–707.
16. Fischer A, Zalvide J, Faurobert E, et al. Cerebral cavernous malformations: from CCM genes to endothelial cell homeostasis. *Trends Mol Med*. 2013;19(5):302–308.
17. You C, Sandalcioglu IE, Dammann P, et al. Loss of CCM3 impairs DLL4-Notch signalling: implication in endothelial angiogenesis and in inherited cerebral cavernous malformations. *J Cell Mol Med*. 2013;17(3):407–418.
18. Zheng X, Xu C, Di Lorenzo A, et al. CCM3 signaling through sterile 20-like kinases plays an essential role during zebrafish cardiovascular development and cerebral cavernous malformations. *J Clin Invest*. 2010;120(8):2795–2804.
19. He Y, Zhang H, Yu L, et al. Stabilization of VEGFR2 signaling by cerebral cavernous malformation 3 is critical for vascular development. *Sci Signal*. 2010;3(116):ra26.
20. Chan AC, Drakos SG, Ruiz OE, et al. Mutations in 2 distinct genetic pathways result in cerebral cavernous malformations in mice. *J Clin Invest*. 2011;121(5):1871–1881.
21. Louvi A, Nishimura S, Gunel M. Ccm3, a gene associated with cerebral cavernous malformations, is required for neuronal migration. *Development*. 2014;141(6):1404–1415.
22. Louvi A, Chen L, Two AM, et al. Loss of cerebral cavernous malformation 3 (Ccm3) in neuroglia leads to CCM and vascular pathology. *Proc Natl Acad Sci U S A*. 2011;108(9):3737–3742.
23. Guerrero A, Iglesias C, Raguz S, et al. The cerebral cavernous malformation 3 gene is necessary for senescence induction. *Aging Cell*. 2015;14(2):274–283.
24. Labauge P, Fontaine B, Neau JP, et al. Multiple dural lesions mimicking meningiomas in patients with CCM3/PDCD10 mutations. *Neurology*. 2009;72(23):2044–2046.
25. Fauth C, Rostasy K, Rath M, et al. Highly variable intrafamilial manifestations of a CCM3 mutation ranging from acute childhood cerebral haemorrhage to late-onset meningiomas. *Clin Neurol Neurosurg*. 2015;128:41–43.
26. El Hindy N, Keyvani K, Pagenstecher A, et al. Implications of Dll4-Notch signaling activation in primary glioblastoma multiforme. *Neuro Oncol*. 2013;15(10):1366–1378.
27. Alajati A, Laib AM, Weber H, et al. Spheroid-based engineering of a human vasculature in mice. *Nat Methods*. 2008;5(5):439–445.
28. Rosa R, Damiano V, Formisano L, et al. Combination of a Toll-like receptor 9 agonist with everolimus interferes with the growth and angiogenic activity of renal cell carcinoma. *Oncoimmunology*. 2013;2(8):e25123.
29. Charalambous C, Chen TC, Hofman FM. Characteristics of tumor-associated endothelial cells derived from glioblastoma multiforme. *Neurosurg Focus*. 2006;20(4):E22.
30. Hoelzinger DB, Demuth T, Berens ME. Autocrine factors that sustain glioma invasion and paracrine biology in the brain microenvironment. *J Natl Cancer Inst*. 2007;99(21):1583–1593.

31. Xie Q, Mittal S, Berens ME. Targeting adaptive glioblastoma: an overview of proliferation and invasion. *Neuro Oncol*. 2014; 16(12):1575–1584.

32. Koochekpour S, Merzak A, Pilkington G. Vascular endothelial growth-factor production is stimulated in response to growth-factors in human glioma-cells. *Oncol Rep*. 1995;2(6): 1059–1061.

33. Munaut C, Noel A, Hougrand O, et al. Vascular endothelial growth factor expression correlates with matrix metalloproteinases MT1-MMP, MMP-2 and MMP-9 in human glioblastomas. *Int J Cancer*. 2003;106(6):848–855.

34. van der Valk P, Lindeman J, Kamphorst W. Growth factor profiles of human gliomas. Do non-tumour cells contribute to tumour growth in glioma? *Ann Oncol*. 1997;8(10):1023–1029.